Convective Flow in Baroclinic Vortices

SERGEY N. ARISTOV* AND JONAS NYCANDER

Department of Technology, Uppsala University, Uppsala, Sweden

(Manuscript received 23 January 1993, in final form 2 July 1993)

ABSTRACT

Convective flow in baroclinic vortices is studied analytically, taking viscosity ν and thermal diffusivity κ into account. The meridional circulation depends strongly on the Prandtl number $\mathrm{Pr} = \nu/\kappa$. If $\mathrm{Pr} > 1$, there is upwelling in the interior of the vortex and the vertical heat diffusion is therefore inhibited by advection. The radial flow is inward in most of the vortex, which is compensated by outward flow in a viscous boundary layer just below the surface. The authors focus on the strongly nonlinear regime, when the background stratification is much weaker than that of the vortex. It is found that the nonlinear equation governing the flow in the limit $\mathrm{Pr} \gg 1$ has a class of exact time-dependent solutions. In this class the evolution of the vertical temperature profile is determined by Burger's equation, whereas the horizontal profile is determined by the Liouville equation. Both these equations can be solved analytically.

1. Introduction

Isolated circular vortices are very common in the oceans (McWilliams 1985; Monin and Zikharev 1990). Their lifetime can be up to several years; thus they can clearly be regarded as stationary to a first approximation in the framework of quasigeostrophic theory. One reason for nonstationarity and slow decay is the radiation of Rossby waves, which has been studied by several authors (Flierl 1984; Korotaev 1988; Hesthaven et al. 1992). It is caused by the β effect, which is quite weak for typical amplitudes and sizes of oceanic vortices. Another reason is viscosity and diffusion of heat (or salt). These dissipational effects give rise to a slow convective (meridional) flow, which is the subject of the present work.

The most important parameter determining the character of the meridional circulation is the Prandtl number, $\mathrm{Pr} = \nu/\kappa$, where ν is the viscosity and κ the thermal diffusivity. In water $\mathrm{Pr} \approx 6$. (The corresponding Schmidt number $\mathrm{Sc} = \nu/\kappa_c$, where κ_c is the salt diffusivity, is about 5000 in the ocean.) However, in a realistic model one should use effective turbulent transport coefficients, which are not very well defined but certainly much larger than the laminar values. The correct value of Pr is then, unfortunately, not known.

The previous study most closely related to the present work is the one by Flierl and Mied (1985). They studied the meridional circulation and gradual decay of a warm core ring analytically and numerically using both large and small Prandtl number ($\mathrm{Pr} = 10$ and 0.1, respectively). In the analytic calculations they used a simplified linear model, which means that the stratification of the density anomaly in the vortex is assumed to be much weaker than the background stratification. The advection of the temperature anomaly can then be neglected, while the advection of the background field is included, just as in the conventional quasigeostrophic approximation. They found that the direction of the meridional circulation depends on whether Pr is larger or smaller than unity.

In their numerical simulations Flierl and Mied used fully nonlinear balance equations (allowing also for a Rossby number of order unity), and judging from their figures the nonlinearity (i.e., the ratio between the stratification of the density anomaly in the vortex and the background stratification) was of the order 10^2. This may be unrealistically large, but the nonlinearity in real vortices can clearly exceed unity (Monin and Fedorov 1983). The simulations confirmed that the direction of the meridional circulation depends on the Prandtl number. They also showed that the vortex decays much faster if $\mathrm{Pr} = 0.1$ than if $\mathrm{Pr} = 10$. This cannot be explained from the linear model.

These results indicate that a particularly interesting case is when both the nonlinearity and the Prandtl number are large. The meridional circulation is then inward and upward in the vortex core, and the advection will oppose the diffusion, prolonging the lifetime of the vortex. In the present article we will derive some analytic results for this regime. Assuming the Rossby number to be small, we find that in the limit $\mathrm{Pr} \gg 1$ the dynamics can be described by a relatively simple

* Permanent affiliation: Institute of Continuum Mechanics, Perm, Russia.

Corresponding author address: Dr. Jonas Nycander, Department of Technology, Uppsala University, Box 534, Uppsala, 751 21 Sweden.

nonlinear equation. Moreover, we find that this equation has a class of nonstationary exact solutions. In this class the vertical dynamics is determined by Burger's equation, which is integrable. The horizontal temperature profile is independent of time and depth, and determined by the Liouville equation, which can also be solved exactly. The solution can have the form of an isolated vortex with no background stratification, which corresponds to large nonlinearity, as in the numerical simulations by Flierl and Mied.

2. Basic equations

We start our considerations from the three-dimensional Boussinesq equations. For large-scale geophysical flows we can use the shallow-water approximation; that is, $H/L \ll 1$, where H is the vertical and L the horizontal length scale. This allows us to replace the vertical component of the equation of motion by the hydrostatic approximation:

$$\frac{\partial p}{\partial z} = g\rho_0 \alpha T, \tag{1}$$

where p and T are the pressure and temperature deviations from a basic state, which is assumed to have constant temperature and density, and α is the volume expansion coefficient defined by $\rho = \rho_0(1 - \alpha T)$, where ρ is the density. In the shallow-water approximation we can also neglect the horizontal viscosity and diffusion, so that the horizontal component of the equation of motion is

$$\frac{d\mathbf{v}_\perp}{dt} + f\mathbf{z} \times \mathbf{v}_\perp = -\frac{\nabla p}{\rho_0} + \nu \frac{\partial^2 \mathbf{v}_\perp}{\partial z^2}. \tag{2}$$

The gradient operator here and below only contains the horizontal components, $\nabla \equiv \mathbf{x}\partial/\partial x + \mathbf{y}\partial/\partial y$, and the Coriolis parameter f is considered constant. The remaining two equations are the incompressibility condition,

$$\nabla \cdot \mathbf{v}_\perp + \frac{\partial w}{\partial z} = 0. \tag{3}$$

where w is the vertical velocity, and the diffusion equation for heat (or salt)

$$\frac{dT}{dt} = \kappa \frac{\partial^2 T}{\partial z^2}. \tag{4}$$

We now assume that the Rossby and Ekman numbers are small, so that Eq. (2) is dominated by the Coriolis term and $\mathbf{v}_\perp$ by the geostrophic velocity:

$$\mathbf{v}_g = \frac{1}{\rho_0 f} z \times \nabla p. \tag{5}$$

Solving Eq. (2) by perturbation theory and including the lowest-order ageostrophic terms, we obtain

$$\mathbf{v}_\perp = \mathbf{v}_g - \frac{1}{\rho_0 f^2} \frac{d_g \nabla p}{dt} + \frac{\nu}{\rho_0 f^2} \frac{\partial^2 \nabla p}{\partial z^2}, \tag{6}$$

where the operator d_g/dt is defined by

$$\frac{d_g}{dt} \equiv \frac{\partial}{\partial t} + \mathbf{v}_g \cdot \nabla = \frac{\partial}{\partial t} + \frac{1}{\rho_0 f} J(p, \cdot),$$

and the Jacobian by $J(f, g) \equiv \partial_x f \partial_y g - \partial_y f \partial_x g$. Substituting Eq. (6) into Eqs. (3) and (4), we obtain

$$\frac{\partial w}{\partial z} = \frac{1}{\rho_0 f^2} \frac{d_g \nabla^2 p}{dt} - \frac{\nu}{\rho_0 f^2} \frac{\partial^2}{\partial z^2} \nabla^2 p, \tag{7}$$

$$\frac{d_g T}{dt} + w\frac{\partial T}{\partial z} + \left(\frac{\nu}{\rho_0 f^2} \frac{\partial^2 \nabla p}{\partial z^2} - \frac{1}{\rho_0 f^2} \frac{d_g \nabla p}{dt} \right) \cdot \nabla T = \kappa \frac{\partial^2 T}{\partial z^2}. \tag{8}$$

The Laplacian in Eq. (7) contains only horizontal derivatives.

Equations (1), (7), and (8) are our basic equations. They must be supplemented by appropriate boundary conditions. At the bottom there is a rigid, no-slip boundary, that is, $w = 0$ and $\mathbf{v}_\perp = 0$. This leads to the formation of an Ekman layer, which ejects fluid into the interior with the pump velocity w_E. Taking the boundary of the domain to lie just above this layer, we obtain the condition

$$w = w_E = \frac{h_E}{2\rho_0 f} \nabla^2 p \quad \text{at} \quad z = -H_0, \tag{9}$$

where $h_E = (2\nu/f)^{1/2}$ is the thickness of the Ekman layer (cf. Gill 1982, p. 331).

We assume the surface to be rigid, so that the barotropic Rossby radius is infinite, which is a good approximation in the cases of interest. However, we cannot use a no-slip condition as at the bottom. Instead, the appropriate boundary condition at a free surface of a viscous fluid is that the normal derivative of the tangential velocity vanishes, that is, $\partial \mathbf{v}_\perp / \partial z = 0$. If there is a horizontal temperature gradient this condition is violated by the thermal wind relation, and a viscous boundary layer is formed. Taking the boundary of the domain to lie just below this layer, the appropriate condition is

$$w = -\frac{g\alpha h_E^2}{2f} \nabla^2 T = -\frac{h_E^2}{2\rho_0 f} \nabla^2 \frac{\partial p}{\partial z} \quad \text{at} \quad z = 0. \tag{10}$$

This condition was used by Flierl and Mied (1985), and a short derivation is given in appendix A.

The temperature changes very little across the boundary layer at the surface; hence if the temperature is held fixed at the water surface, the same boundary condition applies at the boundary of the domain, just below the boundary layer. The heat flux, on the other hand, varies significantly across this layer, which leads to a jump condition for the vertical temperature gradient:

$$\left.\frac{\partial T}{\partial z}\right|_{\text{surface}} - \left.\frac{\partial T}{\partial z}\right|_{z=0-} = -\frac{g\alpha h_E^2}{2\kappa f}(\nabla T)^2, \quad (11)$$

where $z = 0-$ is a point just below the boundary layer. This result is also derived in appendix A. The additional heat flux is due to the temperature advection by the radial flow in the boundary layer. Thus, if the boundary condition at the surface involves heat flux, the corresponding condition at the boundary of the domain is modified. Finally, there are no boundary conditions for the pressure.

Equations (1), (7), and (8) contain a number of different dynamical regimes, with different typical timescales. For instance, in the isothermal case, $T = 0$, Eq. (1) shows that $\partial p/\partial z = 0$, and it then follows from Eq. (7) that w is a linear function of z. The coefficients of this function are determined by the boundary conditions (9)–(10), and Eq. (7) is reduced to

$$\frac{1}{f}\frac{d_g}{dt}\nabla^2 p = -\frac{h_E}{2H_0}\nabla^2 p. \quad (12)$$

This is the barotropic vorticity equation with bottom friction included. The fastest timescale is usually given by the advective term on the left-hand side, while the right-hand side results in a spindown time τ_E given by

$$\tau_E^{-1} \sim \frac{f h_E}{2H_0}. \quad (13)$$

Another special case contained in Eqs. (1), (7), and (8) is the three-dimensional quasigeostrophic potential vorticity equation [Eq. (12.8.7) in Gill (1982)]. To obtain this, one assumes that the background stratification $T_0(z)$ is strong and neglects the nonlinear advection terms in Eq. (8), while keeping the term $wT_0'(z)$.

3. Derivation of the reduced equation

We are interested in circular vortices, where the nondissipative dynamics (described by the quasigeostrophic potential vorticity equation) is stationary. In this case the Jacobians in the advective terms in Eqs. (7) and (8) vanish identically, and d_g/dt can everywhere be replaced by $\partial/\partial t$. The equations then still describe two kinds of processes with different timescales. The first one is the spindown of the barotropic component with the timescale (13). The second one is baroclinic diffusion and convection, which is the main subject of the present work.

We must first understand how the two kinds of dissipational processes can be separated. The timescale τ_κ for baroclinic diffusion and convection is determined by Eq. (8):

$$\tau_\kappa^{-1} \sim \frac{\kappa}{H^2} \sim \frac{f h_E^2}{2H^2}\text{Pr}^{-1}. \quad (14)$$

Here H is the vertical scale of the baroclinic vortex (which may be much smaller than the total depth H_0), and $\text{Pr}^{-1} = \kappa/\nu$ is the inverse Prandtl number. We will assume Pr^{-1} to be small. Compare the timescales for diffusion and barotropic spindown:

$$\frac{\tau_\kappa^{-1}}{\tau_E^{-1}} \sim \frac{h_E H_0}{H^2}\text{Pr}^{-1}. \quad (15)$$

This means that unless the vortex is very shallow (i.e., H/H_0 very small), the spindown is much faster than the diffusive processes. We then have approximately $\partial T/\partial t = \partial/\partial z(\partial p/\partial t) = 0$ during spindown. Thus, the pressure perturbation decreases uniformly at all depths, until it is zero at the bottom and the Ekman pumping ceases. The barotropic component has then vanished, and we can consider the baroclinic mode in isolation. Alternatively, if the vortex is so shallow that the ratio (15) is large, we simply assume that the initial amplitude of the barotropic mode is so small that it can be neglected.

To check that it is consistent to neglect the pressure perturbation p_b at the bottom, we then estimate the bottom pressure induced by the baroclinic mode. Integrating Eq. (7) from $z = -H_0$ to $z = 0$ and using the boundary conditions (9) and (10), we obtain

$$\nabla^2 p_b = -\frac{2}{h_E f}\int_{-H_0}^{0}\nabla^2\frac{\partial p}{\partial t}dz, \quad (16)$$

assuming that the temperature perturbation is zero at the bottom. If the perturbation is localized in the xy plane, the Laplacian is invertible and may be removed from both sides of Eq. (16). Using Eq. (1) it can then be written as

$$\left(1 + \frac{2H_0}{f h_E}\frac{\partial}{\partial t}\right)p_b = -\frac{2g\rho_0\alpha}{h_E f}\int_{-H_0}^{0}dz\int_{-H_0}^{z}\frac{\partial T}{\partial t}dz'. \quad (17)$$

The second term on the left-hand side here comes from the boundary condition at $z = -H_0$ when integrating Eq. (1) and describes spindown of the barotropic mode. If the ratio (15) is small, this term just results in a small time lag, while the right-hand side of (17) gives the bottom pressure excited by the baroclinic mode. We can estimate its magnitude as

$$p_b \sim \frac{g\rho_0\alpha}{h_E f}H^2\tau_\kappa^{-1}T.$$

Estimating the typical pressure perturbation in the baroclinic vortex as $p \sim Hg\rho_0\alpha T$, we obtain

$$\frac{p_b}{p} \sim \frac{h_E}{2H}\text{Pr}^{-1}. \quad (18)$$

Thus, the induced bottom pressure is small compared to the baroclinic pressure perturbation; that is, the vertical viscosity and diffusion drive the vortex flow toward compensation. Also notice that the zero-angular-momentum condition for steady translation on the beta-plane found by Flierl et al. (1983) would require $p_bH_0/(pH) \sim 1$, that is, that the ratio (15) is of order unity.

We should also compare the typical baroclinic vertical velocity w with the barotropic vertical velocity w_{bt} caused by the Ekman pumping (and evaluated at the vortex). Estimating w from the last term in Eq. (7), which is the dominating term for the baroclinic mode, we obtain

$$\frac{w_{bt}}{w} \sim \frac{H^2}{4h_E H_0}\frac{p_b}{p} \sim \frac{H}{2H_0}\,\mathrm{Pr}^{-1}. \tag{19}$$

Thus, assuming Pr^{-1} to be small, we can neglect the vertical velocity due to the Ekman pumping, and set $p_b = 0$. (However, this is not true if Pr^{-1} is of order unity or larger, unless the vortex is very shallow.)

Using the timescale τ_κ^{-1} from (14), we can also compare the two terms on the right-hand side of Eq. (7). It is found that the ratio between them is of the order Pr^{-1}, so that the first term can be neglected. [From Eq. (17) it is also seen that this approximation is consistent with $p_b = 0$.] Equation (7) can then be integrated, assuming $T = 0$ at the bottom:

$$w = -\frac{g\alpha\nu}{f^2}\nabla^2 T, \tag{20}$$

where we have used Eq. (1). This result is then substituted into Eq. (8). In that equation we may also neglect the term $\partial(\nabla p)/\partial t \cdot \nabla T$, since it is smaller than the first term of the equation by the Rossby number. The result is

$$\frac{\partial T}{\partial t} = -\frac{\nu g\alpha}{f^2}\left(\frac{\partial \nabla T}{\partial z}\cdot\nabla T - \nabla^2 T\frac{\partial T}{\partial z}\right) + \kappa\frac{\partial^2 T}{\partial z^2}, \tag{21}$$

which is our final dynamic equation. In the planar case (for a straight front) it has earlier been obtained by Gill (1981) and Garrett (1982). The first and second terms on the right-hand side describe the effect of horizontal and vertical advection, respectively. For the lifetime of the vortex to be much longer than the linear estimate, these advection terms should almost compensate the diffusion (the last term). This condition leads to the order-of-magnitude estimate

$$\mathrm{Ro} \sim \frac{\Omega}{f} \sim \mathrm{Pr}^{-1}, \tag{22}$$

where Ro is the Rossby number and Ω the vorticity. Thus, if Pr^{-1} is small, the Rossby number is also small. The same condition can be expressed in terms of the baroclinic Rossby radius r_R, defined by

$$r_R^2 \sim \frac{g'H}{f^2} \sim \frac{g\alpha TH}{f^2},$$

where g' is the reduced gravity. The horizontal scale L of the vortex can then be estimated as

$$L \sim r_R\,\mathrm{Pr}^{1/2}. \tag{23}$$

Thus, the vortex is larger than the baroclinic Rossby radius.

We finally summarize the scaling region in which Eq. (21) is valid. The appropriate scaling is $\mathrm{Ro} \sim \mathrm{Pr}^{-1} \ll 1$, $\partial/\partial t \sim \kappa/H^2$, and $\mathrm{Ek} \ll 1$, where $\mathrm{Ek} \sim \nu/fH^2$ is the Ekman number. The ratio between Ro and Ek is arbitrary. [In fact, Eq. (21) is valid without the restriction to circular symmetry if $\mathrm{Ro} \ll \mathrm{Ek}$, and then describes the general three-dimensional dynamics. However, in oceanographic applications we of course usually have Ro > Ek.] To estimate the bottom pressure and separate the baroclinic and barotropic modes, we also have to make some assumption for H/H_0, the depth of the vortex compared with that of the ocean. From (15) and (19) it can be seen that anything between $H/H_0 \sim (\mathrm{Ek})^{1/2}$ and $H/H_0 \sim 1$ will do.

To clarify the relation between the present work and that by Flierl and Mied, we now derive a diagnostic equation, similar to their Eq. (4′) or (5), from Eqs. (1), (7), and (8). We first introduce the field η, defined by $w = \nabla^2\eta$. For localized solutions the Laplacian is invertible and can be removed from all terms in Eq. (7). We then take the time derivative of Eq. (1) and eliminate all time derivatives by using Eqs. (7) and (8). The resulting equation can be written

$$\frac{f^2}{g\alpha}\frac{\partial^2\eta}{\partial z^2} + \frac{\partial T}{\partial z}\nabla^2\eta - \nabla T\cdot\frac{\partial\nabla\eta}{\partial z} = (\kappa - \nu)\frac{\partial^2 T}{\partial z^2}. \tag{24}$$

Both in this equation and in Eqs. (4′) and (5) of Flierl and Mied, the Rossby number is small. However, they differ in two other ways. First, Flierl and Mied included horizontal diffusive processes, which have here been neglected. Second, and more important, they neglected both the advection terms on the left-hand side of Eq. (24), except the vertical advection of the background temperature field, which gives a term proportional to $N^2\nabla^2\eta$. (Here N is the buoyancy frequency.) In this way they obtained a simple linear equation for the meridional circulation, driven by the temperature field (or, equivalently, by the azimuthal velocity) on the right-hand side.

In the strongly nonlinear case, this diagnostic equation is generally less useful. Even the case Pr = 1 (in which the right-hand side vanishes) is nontrivial, since the meridional circulation is still driven by the viscous boundary layer at the surface [cf. Eq. (10)]. Therefore, $\eta = 0$ is no solution unless we neglect the vertical viscosity. (Flierl and Mied assumed the horizontal viscosity to be much larger than the vertical one.)

For $\mathrm{Pr} \gg 1$, however, the first term on the left-hand side and the last term on the right-hand side of Eq. (24) are larger than the others. Thus, in this case the equation reduces to Eq. (20), and we again obtain a simple diagnostic equation.

4. Exact solutions

We will now examine a class of exact solutions to Eq. (21) that can be found by separation of variables:

$$T = \Theta(r)F(t, z). \quad (25)$$

Substituting (25) into Eq. (21) and setting the separation constant equal to $1/r_0^2$, where r_0 is an arbitrary length that will be chosen as the vortex radius, we obtain

$$\frac{\partial F}{\partial t} + \frac{\nu g \alpha}{r_0^2 f^2} F \frac{\partial F}{\partial z} = \kappa \frac{\partial^2 F}{\partial z^2}, \quad (26)$$

$$\left(\frac{\partial \Theta}{\partial r}\right)^2 = \Theta\left(\frac{1}{r_0^2} + \frac{1}{r}\frac{\partial}{\partial r} r \frac{\partial \Theta}{\partial r}\right). \quad (27)$$

Equation (26) is Burger's equation, which is known to be integrable. In appendix B it is shown that Eq. (27), which determines the horizontal profile of the vortex, can be integrated also. One solution is

$$\Theta = \begin{cases} \frac{1}{8}[1 - (r/r_0)^2], & r < r_0 \\ 0, & r > r_0 \end{cases} \quad (28)$$

(cf. Fig. 1). The maximum azimuthal velocity is at $r = r_0\sqrt{3}$. The solution is continuous up to the first derivative, whereas the second derivative is discontinuous at r_0. This means that the heat flux and the radial velocity are continuous, while the vertical velocity w is discontinuous, according to Eq. (20). This is permissible since we have neglected the horizontal viscosity. In reality it will presumably lead to the formation of a boundary layer whose width is of the same magnitude as the height H of the vortex. Since this is much smaller than the horizontal scale L of the whole vortex, it can be neglected in the lowest-order approximation.

For a baroclinic vortex with the horizontal temperature profile given by (28), the vertical evolution is determined by Burger's equation. Qualitatively, a solution of this equation will sharpen its profile at places where $\partial F/\partial z$ is negative, until a chock front appears that propagates steadily upward. However, $\partial F/\partial z < 0$ means that the fluid is unstably stratified, since $\Theta > 0$, and such a flow will therefore quickly be disrupted by Rayleigh–Taylor type instabilities. Physically realizable flows must have $\partial F/\partial z > 0$ everywhere, and the profile will then in general tend to become smoother.

To solve Burger's equation, we introduce the function

$$\phi = \exp\left(-\frac{p'}{2}\right), \quad (29)$$

where p', defined by $\partial p'/\partial z = (\nu g \alpha/\kappa r_0^2 f^2)F$, can be thought of as normalized pressure. [To get the full pressure field we must of course multiply by $\Theta(r)$.] We

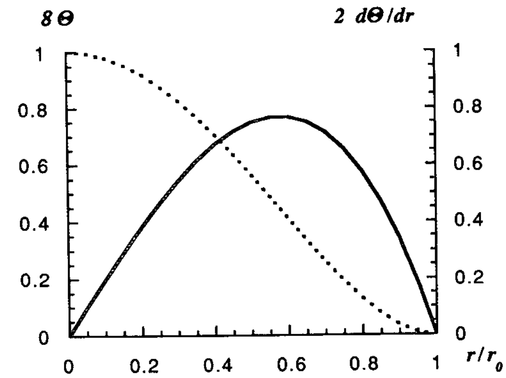

FIG. 1. Radial profile of the temperature and the azimuthal velocity [from Eq. (28)]: $\Theta(r)$ (dotted) is proportional to the temperature, and $\Theta'(r)$ (solid) to the velocity; r_0 is the vortex radius.

assume that the depth of the ocean is infinite, and that $p' \to 0$ as $z \to -\infty$. Using Eq. (29), (26) is transformed to the linear diffusion equation

$$\frac{\partial \phi}{\partial t} = \kappa \frac{\partial^2 \phi}{\partial z^2}, \quad (30)$$

which can be solved by standard methods. Then F is obtained from the relation

$$F = -2\frac{\kappa r_0^2 f^2}{\nu g \alpha}\frac{\phi_z}{\phi}. \quad (31)$$

For illustration, we solve Eq. (26) with the boundary condition $F = F_0$ at $z = 0$, which gives the following boundary condition for ϕ:

$$\frac{\partial \phi}{\partial z} + C\phi = 0 \quad \text{at} \quad z = 0, \quad (32)$$

where

$$C = \frac{\nu g \alpha}{\kappa r_0^2 f^2}\frac{F_0}{2}.$$

The general solution of Eq. (30) with this boundary condition, and the initial value $\phi = f(z)$ at $t = 0$ and $z < 0$, can be found by Fourier transformation:

$$\phi = \frac{1}{2\sqrt{\pi\kappa t}}\int_{-\infty}^{0} d\xi f(\xi)\left[\exp\left(-\frac{(z+\xi)^2}{4\kappa t}\right) + \exp\left(-\frac{(z+\xi)^2}{4\kappa t}\right) - 2C\int_{-\infty}^{0}\exp\left(-\frac{(z+\xi+\zeta)^2}{4\kappa t} + C\zeta\right)d\zeta\right].$$

The simplest case is $f = 1$, corresponding to $F = 0$. The solution can then be written

$$\phi = -\mathrm{erf}\left(\frac{z}{2\sqrt{\kappa t}}\right) + \exp(C^2\kappa t - Cz)\left[1 + \mathrm{erf}\left(\frac{z - 2C\kappa t}{2\sqrt{\kappa t}}\right)\right],$$

where erf is the error function. Using Eq. (31), we finally obtain

$$F = F_0\left[1 - \frac{\mathrm{erf}\left(\frac{z}{2\sqrt{\kappa t}}\right)\exp(Cz - C^2\kappa t)}{1 + \mathrm{erf}\left(\frac{z - 2C\kappa t}{2\sqrt{\kappa t}}\right)}\right]^{-1}. \quad (33)$$

Physically, this solution describes how a vortex is excited by heating the surface. Its behavior in various asymptotic regimes can easily be understood. There is a characteristic time $t_c = 1/(\kappa C^2)$, and for $t \ll t_c$ it may be shown that the solution is approximately

$$F \approx F_0\left[1 + \mathrm{erf}\left(\frac{z}{2\sqrt{\kappa t}}\right)\right]. \quad (34)$$

This is the solution of the linearized version of Eq. (26), with the same boundary condition and initial value. Thus, before t_c the meridional circulation is still too weak to affect the development, and the heat is simply diffusing downward. For $t \gg t_c$, the heat advection is very important. There are then two different asymptotic depth regions. At $z \gg -(\kappa t)^{1/2}$ (i.e., small depth) we obtain

$$F \approx \frac{F_0}{1 - Cz}. \quad (35)$$

Thus, the upper part of the vortex is stationary, and heat advection and diffusion almost exactly balance. At $z \ll -(\kappa t)^{1/2}$ we obtain, using the asymptotic expansion of the error function,

$$F \approx \frac{2F_0}{2C\kappa t - z}\left(\frac{\kappa t}{\pi}\right)^{1/2}\exp\left(-\frac{z^2}{4\kappa t}\right). \quad (36)$$

This describes a diffusive front, where advection is not yet important. It has two subregions. For $z \ll -C\kappa t$ the solution is the same as the linear solution, obtained by asymptotic expansion of Eq. (34). In the subregion $-C\kappa t \ll z \ll -(\kappa t)^{1/2}$, the solution is curiously enough independent of the surface temperature F_0.

In Fig. 2 we have plotted the solution (33), both before and after t_c. We also show the linear, purely diffusive solution (34) at the same value of t, and the stationary solution (35). The general development is that the full solution (33) follows the linear solution until this crosses the stationary curve. After that (33) is approximately equal to the smallest of the linear and the stationary solutions, and everywhere smaller than both.

The pressure perturbation at the surface increases logarithmically with the depth of the stationary region,

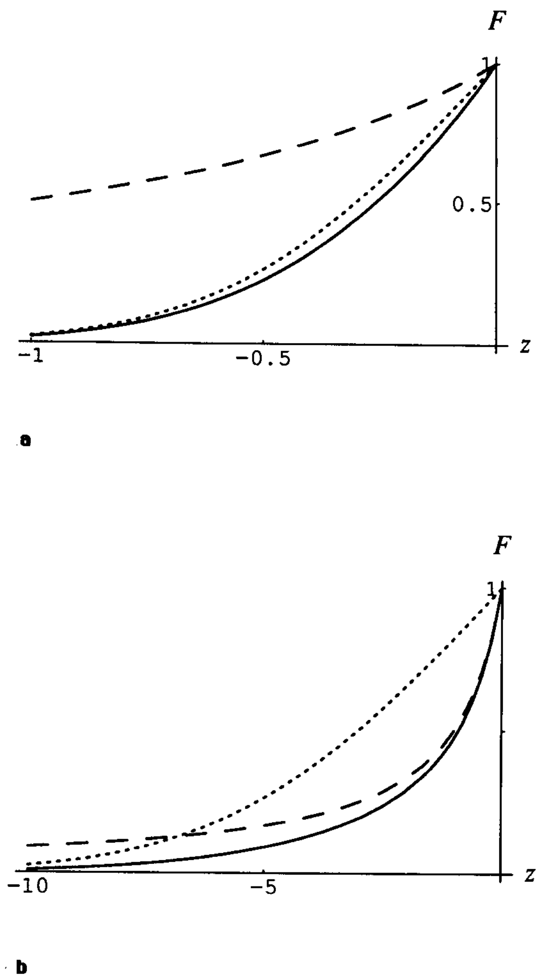

FIG. 2. Plot of the exact solution (33) (solid curve). We also show the linear, purely diffusive solution (34) (dotted) and the stationary solution (35) (dashed). The values used are $C = F_0 = \kappa = 1$, which gives $t_c = 1$: (a) $t = 0.1\ t_c$; (b) $t = 10\ t_c$.

as can be seen by integrating Eq. (35). Thus, in an infinitely deep ocean, the solution cannot be stationary everywhere, and the vertical diffusion cannot be completely canceled by advection, even when the Prandtl number and the nonlinearity are large. In the initial stage of the solution (33), before t_c, the surface pressure increases as $\sqrt{t}$. After t_c it grows more slowly, $\sim\log(t)$, but without bound. At some time the azimuthal velocity and the Rossby number therefore become too large for the model to be valid. The reason for this is of course that the surface is heated in this problem. If there is no heat flux into the vortex, the surface pressure can only decrease.

The meridional flow and the isotherms in the baroclinic vortices studied here are shown qualitatively in Fig. 3. Notice that the radial velocity is inward (toward the center of the vortex) everywhere in the interior of the fluid. This is compensated by an outward flow in

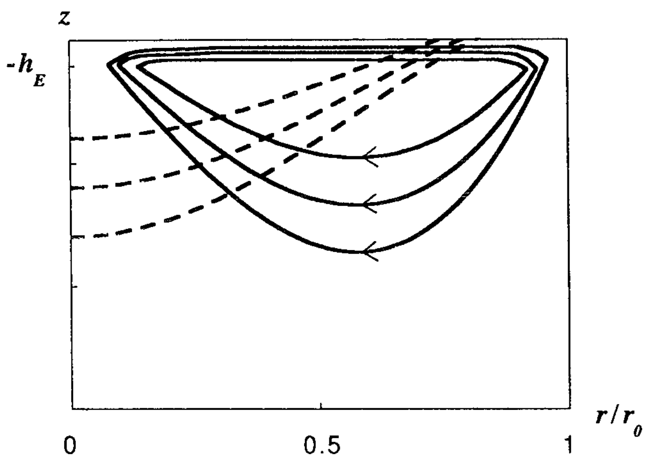

FIG. 3. Qualitative structure of the vortex, where h_E is the thickness of the Ekman layer at the surface and H the vortex depth (i.e., the depth of the thermocline). Solid curves: streamlines of the meridional flow; dashed curves: isotherms.

the boundary layer near the surface. This requires, of course, that the radial velocity is much larger in the boundary layer, and from the solution given in appendix A it may be estimated that it is indeed larger than the radial velocity in the interior by the factor H/h_E. Nevertheless, it is still smaller than the geostrophic azimuthal velocity by the same factor.

Since $T = 0$ for $r > r_0$, there is no background stratification in the exact solution given here. In the presence of background stratification, we set $T = T_0(z) + T_1$ in Eq. (21), and obtain the same equation for the temperature anomaly T_1, but now with an additional term that looks exactly like horizontal diffusion, as was pointed out by Gill (1981). Separation of variables as in Eq. (25) is then impossible. The reason is clearly that some horizontal spreading of the temperature anomaly will occur, so that the radial profile changes in time. Physically, this spreading is not caused by horizontal diffusion (which we have neglected) or horizontal advection, but rather by the vertical advection of the background temperature field.

5. Discussion

In this paper we have studied dissipational processes and the induced meridional flow in circular baroclinic vortices. This is one of the main candidates for an explanation of the gradual decay of the vortices. (The other one is radiation of Rossby waves.) These processes also determine the evolution of the vertical structure of vortices, for example, the profile of the thermocline and the relative importance of the barotropic and baroclinic modes. In the framework of ideal, dissipationless theory, the vertical structure is arbitrary, and simply determined by the initial conditions.

Our analysis has shown that unless the vortex is very shallow compared to the total depth of the ocean, or the Prandtl number small, the spindown of the barotropic component is much faster than the diffusion time for the baroclinic mode [cf. (15)]. We also found that after the barotropic spindown time has passed, the pressure excited by the baroclinic mode is much smaller at the bottom than in the interior of the vortex [cf. (18)]. That is, the vertical viscosity and diffusion drive the flow toward compensation. Nevertheless, the contribution from the Ekman pumping at the bottom to the meridional circulation cannot be neglected unless the Prandtl number is large, or the vortex very shallow [cf. (19)].

The major simplifying assumption in our subsequent analysis was that the Prandtl number is large. The meridional flow in the vortex core is then upward and inward, so that the advection opposes the diffusion. If the nonlinearity (i.e., the ratio between the stratification of the density anomaly in the vortex and the background stratification) is also large, this can result in a substantially longer lifetime of the vortex, as is seen in the simulations by Flierl and Mied (1985). We focused on this regime and found that in the limiting case (with zero background stratification) there exists a class of exact, nonlinear time-dependent solutions. The horizontal profile of the vortex is then given by Eq. (28), while the vertical profile is determined by Burger's equation, Eq. (26), which is integrable. We have also shown an explicit example of such an exact, time-dependent solution.

Although the simplifying assumptions are perhaps not entirely realistic, this result should serve as a valuable reference point for future modeling. It also has intrinsic interest, being perhaps the first case where the profile of the thermocline can be determined analytically and self-consistently in a nonlinear convection problem.

Acknowledgments. This work was performed while one of the authors (SNA) was a guest at the Department of Technology in Uppsala. He is grateful to the Swedish Institute for the support that made this possible.

APPENDIX A

Viscous Boundary Layer at the Free Surface

When solving the problem for the viscous boundary layer, we can approximate the equation of motion (2) by

$$f\mathbf{z} \times \mathbf{v}_\perp = -\frac{\nabla p}{\rho_0} + \nu \frac{\partial^2 \mathbf{v}_\perp}{\partial z^2}. \tag{A1}$$

We have here neglected the term $d\mathbf{v}_\perp/dt$, since the main ageostrophic contribution in the thin boundary layer is the viscous term. (The neglected term would merely result in a slight change of the functional relation between the azimuthal velocity and the pressure.) The velocity may then be decomposed into the slowly varying geostrophic velocity $\mathbf{v}_g$, which dominates in the interior, and is approximately constant within the boundary layer, and the rapidly varying boundary contribution $\tilde{\mathbf{v}}$, that is, $\mathbf{v}_\perp = \mathbf{v}_g + \tilde{\mathbf{v}}$. The equation for the rapidly varying part is

$$\mathbf{z} \times \tilde{\mathbf{v}} = \frac{\nu}{f}\frac{\partial^2 \tilde{\mathbf{v}}}{\partial z^2}, \quad \text{(A2)}$$

which is the same as in the usual Ekman layer at the bottom. The boundary condition at the surface is $\partial \mathbf{v}_\perp / \partial z = 0$; that is,

$$\frac{\partial \tilde{\mathbf{v}}}{\partial z} = -\frac{\partial \mathbf{v}_g}{\partial z} = -\frac{\alpha g}{f}\mathbf{z} \times \nabla T \quad \text{at} \quad z = 0, \quad \text{(A3)}$$

where we have used the hydrostatic approximation (1). The right-hand side of Eq. (A3) is the thermal wind, which gives a vertical dependence of the geostrophic velocity if there is a horizontal temperature gradient. This thermal wind must be compensated at the surface by the boundary-layer contribution to satisfy the boundary condition. The other boundary condition is $\tilde{\mathbf{v}} \to 0$, $z \to -\infty$. Equation (A2) then has the unique solution

$$\tilde{\mathbf{v}} = \frac{g\alpha}{f}\frac{e^{kz}}{2k}[(-\mathbf{z} \times \nabla T|_{z=0} - \nabla T|_{z=0})\cos(kz) + (-\mathbf{z} \times \nabla T|_{z=0} + \nabla T|_{z=0})\sin(kz)], \quad \text{(A4)}$$

where $k = h_E^{-1} = (f/2\nu)^{1/2}$. Notice that at the surface one velocity component is directed from warm toward cold regions. The incompressibility condition gives

$$\frac{\partial w}{\partial z} = -\nabla \cdot \tilde{\mathbf{v}} = \frac{g\alpha}{f}\nabla^2 T|_{z=0}\frac{1}{2k^2}\frac{d}{dz}(\cos(kz)e^{kz}). \quad \text{(A5)}$$

Integrating this with the boundary condition $w = 0$ at $z = 0$, we obtain

$$w = -\frac{g\alpha h_E^2}{2f}\nabla^2 T|_{z=0} \quad \text{for} \quad kz \ll -1, \quad \text{(A6)}$$

which gives the vertical velocity below the boundary layer. This is the analog of Ekman pumping at a free surface (and should of course not be confused with the Ekman pumping caused by wind forcing).

We also calculate the temperature profile in the boundary layer. We first decompose the temperature into the slowly varying component T_i in the interior of the vortex, and the boundary layer contribution $\tilde{T}$, which is much smaller than T_i and varies on the scale h_E. To lowest order the temperature equation (4) in the boundary layer then takes the form

$$\kappa \frac{\partial^2 \tilde{T}}{\partial z^2} = \tilde{\mathbf{v}} \cdot \nabla T_i, \quad \text{(A7)}$$

where we have neglected the vertical heat advection in comparison with the horizontal one, since the radial velocity is much larger in the boundary layer than in the interior of the vortex. Integrating Eq. (A7) across the boundary layer, using the result (A4), we obtain

$$\frac{\partial \tilde{T}}{\partial z} = -\frac{g\alpha h_E^2}{2\kappa f}(\nabla T_i)^2 e^{kz}\cos(kz), \quad \text{(A8)}$$

where T_i on the right-hand side can be approximated by the total temperature T. We see that there is a jump in the vertical temperature gradient across the boundary layer.

We also remark that if the horizontal temperature gradient is constant, the analogous problem can be solved exactly, without the boundary layer approximation (Aristov and Frick 1988).

APPENDIX B

Solution of the Equation for the Radial Profile

To solve Eq. (26) we first make the transformation

$$\Theta = \frac{r^2}{r_0^2}\Phi(\xi), \quad \text{(B1)}$$

where $\xi = \ln(r/r_0)$. The equation becomes

$$\left(\frac{\partial \Phi}{\partial \xi}\right)^2 = \Phi\left(1 + \frac{\partial^2 \Phi}{2\xi^2}\right). \quad \text{(B2)}$$

We then make the substitution

$$\Phi = Ae^{\Psi}, \quad \text{(B3)}$$

which transforms Eq. (B2) into the one-dimensional Liouville equation (Bateman 1944):

$$\frac{\partial^2 \Psi}{\partial \xi^2} = \frac{e^{-\Psi}}{A}. \quad \text{(B4)}$$

After multiplying by $\partial \Psi / \partial \xi$ it can easily be integrated, giving

$$\left(\frac{\partial \Psi}{\partial \xi}\right)^2 = \frac{2e^{-\Psi}}{A} + C, \quad \text{(B5)}$$

where C is an integration constant. Equation (B5) can be integrated by elementary methods. We get a number of different cases depending on the signs of A and C. We do not show all of them here, but note that for none of them $\Theta(r)$ is localized, or even bounded. Choosing the integration constant in the most convenient way (without loss of generality since r_0 is arbitrary), and transforming back to $\Theta(r)$, two of the solutions can be written

$$\Theta = \frac{1}{8}\left[1 - \left(\frac{r}{r_0}\right)^2\right]^2, \quad \text{(B6)}$$

where r_0 is arbitrary, and

$$\Theta = \frac{r^2}{2r_0^2 K^2}\cos^2\left[K \ln\left(\frac{r}{r_0}\right)\right], \quad \text{(B7)}$$

where r_0 and K are arbitrary. Notice that the solutions touch the r axis smoothly, so that it is possible to match different solutions at these points and still have Θ continuous up to the first derivative. [The reason is that Eq. (27) is singular at $\Theta = 0$.] In this way it is possible to construct a localized vortex from the solution (B6), and vortex rings from (B7).

REFERENCES

Aristov, S. N., and P. G. Frick, 1988: Large-scale turbulence in a thin layer of nonisothermal rotating fluid. *Izv. Akad. Nauk SSSR, Mekh. Zhidk. i Gaza,* **4,** 48–55.

Bateman, H., 1944: *Partial Differential Equations of Mathematical Physics.* Dover, 522 pp.

Flierl, G. R., 1984: Rossby wave radiation from a strongly nonlinear warm eddy. *J. Phys. Oceanogr.,* **14,** 47–58.

——, and R. P. Mied, 1985: Frictionally induced circulations and spin down of a warm-core ring. *J. Geophys. Res.,* **90,** 8917–8927.

——, M. E. Stern, and J. A. Whitehead, Jr., 1983: The physical significance of modons: Laboratory experiments and general integral constraints. *Dyn. Atmos. Oceans,* **7,** 233–263.

Garrett, C., 1982: On spindown in the ocean interior. *J. Phys. Oceanogr.,* **12,** 989–993.

Gill, A. E., 1981: Homogeneous intrusions in a rotating stratified fluid. *J. Fluid Mech.,* **103,** 275–295.

——, 1982: *Atmosphere-Ocean Dynamics.* Academic Press, 662 pp.

Hesthaven, J. S., J. P. Lynov, J. J. Rasmussen, and G. G. Sutyrin, 1993: Generation of tripolar vortical structures on the beta-plane. *Phys. Fluids A,* **5,** 1674–1678.

Korotaev, G. K., 1988: *Theoretical Modelling of Synoptic Variability in the Ocean* (in Russian). Naukova Dumka, 158 pp.

McWilliams, J. C., 1985: Submesoscale, coherent vortices in the ocean. *Rev. Geophys.,* **23,** 165–182.

Monin, A. S., and K. N. Fedorov, 1983: Poloidal circulation in rings. *Dokl. Akad. Nauk SSSR,* **270,** 1213–1216.

——, and G. M. Zikharev, 1990: Ocean eddies. *Sov. Phys. Usp.,* **33,** 313–339. First published in *Usp. Fiz. Nauk,* **160,** 1–47, 1990.